Continuous time quantum walks and the quantum kicked rotor

AUTHOR
Anantha S Rao
20181044

IV BS-MS student, IISER Pune

SUPERVISOR
Prof. MS Santhanam

Division of Physics, IISER Pune

PHY402: Semester project report
January 2022 - May 2022

Contents

1 Abstract

The quantum kicked rotor (QKR) is a quintessential model for quantum chaos in floquet systems, with potential applications in quantum computing and quantum sensor development. In this semester project report, we investigate the relation between the evolution of the QKR at quantum resonance conditions and a continuous-time quantum walk in one dimension. We show that the dynamics of a quasi-periodic rotor at resonance can be realised by temporally varying the transition probabilities of a continuous-time quantum walk. This correspondence can be used to engineer initial states of a QKR to realise experimentally relevant distributions for downstream quantum information processing. To probe the quantum advantage by using the QKR as a system for search algorithms, we use a projective measurement approach to investigate the statistics of first detection times (FDT) with the detector placed at desired target sites. For the QKR-continuous-time quantum walk, the probability of first detection decays like $(\text{time})^{-3}$ with superimposed oscillations, while in the classical random walk, the FDT distribution decays monotonically like $(\text{time})^{-\frac{3}{2}}$. We further show that this advantage can be suppressed in the presence of noisy kicks.

2 Introduction

Periodically driven physical systems have been extensively used to study various phenomena in nonlinear dynamics, quantum chaos, atomic physics, condensed matter physics, and quantum information. The classical kicked rotor model, representing a particle constrained to move along a ring with a time-periodic gravitational kick, can be non-dimensionalized and mapped to the standard (Chirikov) map, which displays a transition from integrability to chaos for K (kicking strength) ≥ 0.97 under periodic boundary conditions in phase-space. The corresponding quantum version, the quantum kicked rotor (QKR) model and its variants, obtained by applying the correspondence principle, yields two non-dimensional parameters: the kicking strength, K, and the scaled plank's constant: $\hbar_s$ [1]. Under stroboscopic, unitary time-evolution, these systems display rich-physical phenomena and can be used to study the origin of quantum chaos, dynamical (or Anderson) localization in condensed matter physics, and recently in the context of quantum information and computation. With the advent of modern, and increasingly precise measurement techniques in atom-interferometry and cold-atoms, it is now possible to conduct experiments to investigate and verify these theoretical predictions.

The theory of Quantum-walks (QWs) plays an essential role in developing novel quantum algorithms. Quantum walks utilize the quantum mechanical postulates of unitary evolution and property of superposition to quantize classical random walks, and under certain conditions, endow a quadratic speed-up over their classical counterpart. Based on the type of temporal evolution, we have discrete-time (DTQW) and continuous-time quantum walks (CTQW), where-in the former uses the notion of position-space and coin-space operators, while the latter solely relies on the unitary evolution of position-space probability amplitudes. There is a deep connection between the dynamics of the QKR and QWs. At resonance conditions, a quantum kicked rotor performs a continuous-time quantum walk in the momentum space with the kicking strength of the QKR linearly proportional to the transition probabilities of a CTQW. In this project, we study the dynamics of a CTQW determined by the hamiltonian of the kicked rotor in one dimension, derive a relation in higher dimensions, explore the advantage of using the quantum kicked rotor as a tool for quantum search protocols, and investigate the quantum advantage using the first-detection time distribution.

3 Kicked Rotor Model

3.1 Classical Kicked rotor

A classical kicked rotor represents a classical point-particle constrained to move on a ring, subjected to periodic gravitational kicking. We model the external kicking as periodic delta function potentials ('Dirac combs'). Between any two successive kicks, the particle undergoes free-particle dynamics. The Hamiltonian of the system is given by:

$$H(p,q,t) = \frac{p^2}{2I} + mgl\cos(q)\sum_{n\in Z^+}\delta(t-n\tau) \tag{1}$$

By non-dimensionalization and setting I=1, this reduces to:

$$H(P,Q,T) = \frac{P^2}{2} + K\cos(Q)\delta_\tau(t)$$

The Hamilton's equation of motion corresponding to the above equation can be found analytically by integration and further discretized as a difference equation (See Appendix 12.1). This difference equation is the standard map or Chirikov map first proposed by Boris Chirikov [2].

$$\begin{aligned} P_{n+1} &= P_n + K\sin Q_n \\ Q_{n+1} &= Q_n + P_{n+1} \end{aligned} \tag{2}$$

Modifying the non-linearity parameter K transitions the system from periodic motion to quasi-periodic, to local chaos (mixed phase-space) and global chaos. The map transforms to be completely chaotic for K > Kc $\sim$ 0.9716, and the diffusion constant (D) is proportional to K^2. A more thorough analysis of the classical kicked rotor is found in [1]

3.2 Quantum Kicked rotor

By applying the correspondence principle to the classical hamiltonian ($p \to \hat{p} = -i\hbar\nabla$) and ($x \to \hat{x}$), the time-independent schrodinger equation for the quantum kicked rotor is given by:

$$\begin{aligned} i\hbar\partial_t\psi(z,t) &= \hat{\mathcal{H}}\psi(z,t) = \left(\mathcal{L}_z^2/2I + V(\theta)\right)\psi(z,t) \\ i\hbar\frac{\partial}{\partial t}\psi(z,t) &= \left(-\frac{\hbar^2}{2I}\frac{\partial^2}{\partial z^2} + k\cos(\theta)\sum_n\delta(t-n\tau)\right)\psi(z,t) \end{aligned} \tag{3}$$

where the operators L_z and θ correspond to the z-component of the angular momentum and the angular direction in the perpendicular plane of the rotor; I is the inertia moment, and τ is the

kicking period. By transforming variables ($t \to \tilde{t}\tau/I$), we can identify two quantum-mechanical parameters, namely, the kicking strength: $\kappa = k/\hbar$ and the scaled Planck's constant $h_s = \hbar\tau/I$. Without loss of generality we can set I=1 and using these scaled units the nondimensional Hamiltonian is given by:

$$\hat{\mathcal{H}} = \frac{\hat{p}^2}{2} + k\cos\hat{x}\delta_1(t) \quad \text{such that } [\hat{x},\hat{p}] = i\hbar_s \tag{4}$$

The periodic nature of the potential endows discrete time-translation symmetry to the problem, and allows us to incorporate floquet theory to describe the unitary dynamics. The evolution operator for one time period $T = 1$, can be described by the Floquet unitary operator $\mathcal{F}$ [3]:

$$\begin{aligned} \mathcal{F} &= \mathcal{U}_{\text{kick}}\mathcal{U}_{\text{free}} = e^{-i\kappa\cos x}e^{-i\hbar_s p^2/2} \\ |\psi(t+1)\rangle &= \mathcal{F}|\psi(t)\rangle \end{aligned} \tag{5}$$

In momentum representation, the eigenvalues of the operator $\hat{p}$ are integer numbers $n \in Z$, and the basis functions are the kets $|n\rangle$ satisfying:

$$\hat{p}|n\rangle = n|n\rangle; \qquad \langle x|n\rangle = \frac{e^{inx}}{\sqrt{2\pi}} \tag{6}$$

Using [5,6], the Floquet operator in the angular momentum basis $\{|n\rangle, |m\rangle\}$ becomes:

$$\begin{aligned} \langle n|F|m\rangle &= \langle n|e^{-i\kappa\cos z}e^{-ip^2/2\hbar_s}|m\rangle = \int_0^{2\pi}\langle n|x\rangle\langle x|e^{-i\kappa\cos x}e^{-ip^2/2\hbar_s}|m\rangle \\ &= \frac{e^{-im^2/2\hbar_s}}{2\pi}\int_0^{2\pi} e^{i(m-n)x}e^{-i\kappa\cos(x)} \\ &= \exp\left(\frac{-i\hbar_s m^2}{2}\right) i^{m-n}J_{m-n}(\kappa) \end{aligned} \tag{7}$$

where $J_n(k)$ is the Bessel function of order $n : J_n(z) = (1/2\pi i^n)\int_0^{2\pi} e^{iz\cos\phi}e^{in\phi}d\phi$.
Two principal phenomena studied with the QKR as a model are the dynamical-localization of the wave function observed in the classically chaotic regime and the condition of quantum resonance. An insight into the former can sought through the observation that the floquet operator is a toeplitz matrix i.e, effectively a banded matrix with the matrix elements $J_{nm}(z) \to 0$ as $|m-n|$ becomes large. The eigenstates of such a matrix exhibit significant contributions from only a narrow band of basis states, implying localized excitations, and localization in momentum basis under time evolution. While extensive literature is available on the former [4, 5], in this work, we are interested to study the later.

3.2.1 Quantum resonances

In the non-dimensionalized hamiltonian of the QKR [4], when $\hbar_s = 4\pi$, the unitary operator that corresponds to free-evolution ($\mathcal{U}_{\text{free}}$) becomes equal to unity, and the evolution is only governed by $\mathcal{U}_{\text{kick}}$. In such a case, the role of $\mathcal{U}_{\text{kick}}$ is to impart an additional phase to any initial state in position basis, such that at every timestep any measurement in the position basis would yield the initial state. Such a condition is called the *primary* quantum resonance. The general case of quantum resonance condition is given by:

$$\hbar_s = 4\pi l; \quad l \in 1, 2, .. \tag{8}$$

The above condition can be physically understood as arising from the following argument: The energy of the unperturbed rotor is $E_n = n^2\hbar^2/2$, where n is the wave number. Transitions between any two unperturbed levels can take place if energy $\Delta E_n = E_{n+1} - E_n = l'\hbar^2/2$ ($l' = 2n + 1$ is an integer) is supplied from an external source that supplies photons with energy $2\hbar/\tau$, where τ is the period of kick. If the energy supplied by l photons matches ΔE_n, then the quantum resonance condition ($\hbar_s = \hbar\tau = 4\pi l/l'$) is satisfied assuming incommensurate l and l'. This is the general condition for quantum resonance, of which Eq 8 is a special case. An operational choice available to achieve quantum resonance is via tuning either the planck's constant $\hbar$ or by tuning kick period τ. Furthermore, at resonance conditions, the quasi-energies (spectrum of the floquet operator) exhibit a continuous spectrum which leads to an unbounded increase in energy with time [6].

If $\hbar_s = (2l+1)2\pi$, then quantum anti-resonance can be observed. In this case, if $n_0 = 2l+1$ is an odd integer, then the time-evolving wavefunction $\psi(x, t)$ acquires a phase that is annihilated at a successive steps. The initial wavefunction is obtained at intervals of one-time step. Under this condition, the mean energy oscillates instead of displaying any growth in time (See Fig(**??**)).

4 Quantum walks

The term "quantum random walks" was first introduced by Y. Aharonov et al., to describe the quantized analogs of classical random walks or classical Markov chains [7]. A classical Markov chain is a stochastic process that assumes values in a discrete set and obeys the Markovian property: the next state of the chain/process only depends on the current state, i.e. it is not influenced by the past states. Based on the nature of the time variable, classical Markov chains can be of two types: (1) Discrete-time Markov chains and (2) Continuous-time Markov chains. By quantizing these markovian chains and allowing for unitary evolution, we can define the quantum versions of these Markov chains: (1) Discrete-time quantum walks and (2) Continuous-time quantum walks.

4.1 Discrete-time quantum walk

The discrete-time quantum walk is the quantum analog of a discrete-time Markov chain or a discrete-time random walker. Before we elucidate the quantum case, we briefly discuss classical random walks. As an example, consider a random walker on a connected-graph: $G = (V, E)$ with n-vertices ($|V| = n$) and e-edges ($|E| = e$). Initially, the walker starts at a particular vertex V_0 with $deg(V_0) = E_0$ and tosses an E_0-dimensional coin. Based on the result of the coin toss, the walker decides to move to another vertex or continues to stay at V_0. At each step, the random walker has an associated probability distribution, which is the set of probabilities of the walker being in the vertices or states. The probability distribution for the location of the random walker at time 't' is described by a vector of the form:

$$[p_1(t), p_2(t), ..., p_n(t)]^T$$

where $p_1(t)$ is the probability of the walker being at vertex x_1 at time t. In a Markov chain, we cannot precisely tell where the walker will be in the future. However, we can determine the probability distribution, if we know the transition matrix $\mathcal{M}$, also called probability matrix or stochastic matrix. If the probability distribution is known at the time 't', we obtain the distribution at time '$t + 1$' by employing the relation: $p(t + 1) = \sum_{j=1}^{n} \mathcal{M}_{ij} p_j(t)$. The matrix $\mathcal{M}$ must satisfy the following properties: all entries must be non-negative real numbers and sum of each column must be equal to 1. In vector form, we have:

$$\vec{p}(t + 1) = \mathcal{M}\vec{p(t)}$$

The quantum walk is constructed by the process of quantization ($p \to -i\hbar\nabla, E \to i\hbar\partial_t$). The state of the quantum system is described by a vector in a Hilbert space and the evolution of the system is unitary. In the quantum case, the walker's position n, labels a vector in a Hilbert space $\mathcal{H}_P$ with the computational basis $\{|n\rangle : n \in Z\}$. The evolution of the walk depends on a "quantum coin" and the associated Hilbert space is $\mathcal{H}_\mathcal{C}$. The Hilbert space of the system is then $\mathcal{H} = H_C \otimes H_P$. At the beginning of the quantum walk,analogous to tossing a coin in the classical case, we apply the coin operator $\mathcal{C}$ to the initial state. $\mathcal{C}$ produces a rotation of the coin state. If the coin is initially described by one of the states of the computational basis, the result may be a superposition of states. Each term in this superposition will generate a shift in one direction. We then apply a conditional-shift operator $\mathcal{S}$ that results in translation in $\mathcal{H}_\mathcal{P}$. For a 1D quantum walk on a line-graph, these operators are given by:

$$U = \mathcal{S}(\mathcal{C} \otimes I) \quad \text{where } \mathcal{S} = |0\rangle\langle 0| \otimes \left(\sum_{n=-\infty}^{\infty} |n + 1\rangle\langle n| \right) + |1\rangle\langle 1| \otimes \left(\sum_{n=-\infty}^{\infty} |n - 1\rangle\langle n| \right)$$

In Fig(3), we observe that quantum walks display ballistic motion. The standard deviation is found to be proportional to time 't'. Furthermore, the probability distribution for the quantum

walk is spread in the interval $[-t/\sqrt{2}, t/\sqrt{2}]$, while the classical distribution is a Gaussian centered at the origin.

4.2 Continuous-time quantum walk

We obtain continuous-time quantum walks by quantizing the classical continuous-time-Markov chains (CTMC). For a CTMC, if the initial distribution is $\vec{p}(0)$ and the transition matrix is $\mathcal{M}$, then $\vec{p}(t)$ is given by: $\vec{p}(t) = \mathcal{M}(t)\vec{p}(0)$ where $\mathcal{M}$ can be written as $\exp(-\mathcal{H}t)$, where $\mathcal{H}$ is called the generator of $\mathcal{M}$. For the quantum case, since evolution is constrained to be unitary, we define the unitary operator as $\mathcal{U}(t) = \exp(-i\mathcal{H}t)$ such that $|\psi(t)\rangle = \mathcal{U}(t)|\psi(0)\rangle$ and the probability density at site 'k': $p_k = |\langle k|\psi(t)\rangle|^2$

Elucidation of a general case:
Consider a random walker on a connected graph $\mathcal{G} = (\mathcal{V}, \mathcal{E})$ where $\mathcal{V}(\mathcal{G})$ is the vertex set and $\mathcal{E}(\mathcal{G})$ is the edge set of the graph $\mathcal{G}$. When time is a continuous variable, the walker can jump from vertices $x_i \to x_j$ given $(x_i, x_j) \in \mathcal{E}(\mathcal{G})$ at any time. We assume a constant transition rate γ between all vertices to immediate neighbours connected its edges (homogenous and isotropic). Consider a time evolution, $t \to t + \epsilon$. If initially at time 't', the walker is at vertex x_i, then at '$t + \epsilon$', the probability that the walker is at one of the x_i's neighbours is $\gamma\epsilon d_i$ where 'd_i' is the degree of vertex x_i. The probability of staying back at x_i is $(1 - d_i\gamma\epsilon)$. In the continuous case, the transition matrix $\mathcal{M}_{ij}(t)$ denotes the probability of a random walker at vertex x_j to go to x_i in a time interval(t). So for an infinitesimal timestep, ϵ, we have eq[9]. We can also define the auxiliary matrix "$\mathcal{H}$" for an infinitesimal timestep 'ϵ', called the generating matrix as the following:

$$M_{ij}(\epsilon) = \begin{cases} 1 - d_j\gamma\epsilon + O(\epsilon^2), & \text{if } i = j \\ \gamma\epsilon + O(\epsilon^2), & \text{if } i \neq j \end{cases} \qquad H_{ij} = \left\{ \begin{array}{ll} d_j\gamma, & \text{if } i = j \\ -\gamma, & \text{if } i \neq j \text{ but } (i,j) \in \mathcal{E}(\mathcal{G}) \\ 0, & \text{if } i \neq j \text{ but } (i,j) \notin \mathcal{E}(\mathcal{G}) \end{array} \right\} \quad (9)$$

Since the process is Markovian, it is possible to show that $\mathcal{M}(t) = e^{-\mathcal{H}t}$ (See Appendix 12.2)
So if $\vec{p}(t) = \mathcal{M}(t)\vec{p}(0)$ then $\vec{p}(t) = e^{-\mathcal{H}t}\vec{p}(0)$. To obtain the quantum analog of the classical walk, we recast the vector that describes the probability distribution to a state vector and the transition matrix to an equivalent unitary operator ($\mathcal{U} = e^{-i\mathcal{H}t}$). If the initial condition is $|\psi(0)\rangle$, the quantum state at time t is $\psi(t) = U(t)\psi(0)$ and the probability distribution is $p_k = |\langle k|\psi(t)\rangle|^2$.

5 Quantum kicked rotor as a continuous-time quantum walk

Consider the case of a continuous-time quantum walk on a line graph. The vertices of such a regular graph can be labelled by integer points and equation [9] reduces to:

$$\mathcal{H}_\gamma = -\gamma \sum_{n=-\infty}^{\infty} |n-1\rangle\langle n| - 2|n\rangle\langle n| + |n+1\rangle\langle n| \tag{10}$$

In Appendix 12.3, we derive an analytical expression for the $\mathcal{H}_\gamma|0\rangle$. Further, using [10], we can compute $\mathcal{U}(t) = e^{-i\mathcal{H}t}$ and the probability distribution at a general time 't'. Here we prove the equivalence between the QKR at the resonant condition and the CTQW on a 1D line. A primary observation is that the QKR's evolution operator at quantum resonance after t kicks can be interpreted as being generated by a Hamiltonian $\mathcal{H}_\kappa = \kappa\cos(\theta)$ acting continuously for a time 't'. Using $\cos\theta = (1/2)(\exp(i\theta) + \exp(-i\theta))$, the similarity with the nearest-neighbour couplings of the CTQW becomes equivalent. Using momentum eigenstates, the Hamiltonian H_k has matrix elements:

$$\langle m|H_k|n\rangle = \frac{1}{2\pi}\int_0^{2\pi} d\theta e^{-im\theta}\kappa\cos\theta e^{-in\theta} \quad = \left\{ \begin{array}{ll} \kappa/2, & \text{if m} = \text{n} \pm 1 \\ 0, & \text{otherwise} \end{array} \right\} \tag{11}$$

Comparing equations [9, 11], for $d_j = 2$, we see that if we choose $\kappa = 2\gamma$, the following relation holds for the CTQW Hamiltonian H_γ and the "effective" kick hamiltonian H_k, at integer t:

$$\bar{\mathcal{H}_\gamma} = 2\gamma\mathcal{I} - \bar{\mathcal{H}_\kappa} \tag{12}$$

We now focus on the probability of being in the n^{th} momentum eigenstate, given the initial state was $|\psi(0)\rangle$, after t kicks of our QKR, we have:

$$\begin{aligned} P_\kappa(n,t) &= |\langle n|U^t|\psi_0|^2 = |\langle n|e^{-iH_\kappa t}|\psi_0\rangle|^2 \\ &= |\langle n|e^{-i(2\gamma\mathcal{I}-H_\gamma t)}|\psi_0\rangle|^2 \\ &= |\langle n|e^{iH_\gamma t)}|\psi_0\rangle|^2 = P_\gamma(n,-t) \end{aligned}$$

The probability $P_\gamma(n,t)$ that the CTQW starting from the same state leads to the same momentum eigenstate is then, for $\gamma = \kappa/2$ and using Equations.

$$P_\gamma(n,t) = P_k(n,-t)$$

Thus, choosing $\gamma = \kappa/2$ produces a CTQW with a time-reversed probability distribution with respect to the evolution induced by the QKR, independent of the initial condition. If $\kappa = 2\gamma$ is chosen instead, the two probability distributions would be equal. Thus the probability distribution of a CTQW, $P_\gamma(n,t)$, is equal to the one of the QKR at resonance, $P_\kappa(n,t)$, at $\kappa = 2\gamma$. Therefore, the simple QKR at principal resonance conditions directly implements a CTQW in the momentum space.

6 CTQW with a time-dependent hamiltonian

The dynamics of a 3-dimensional kicked rotor can be realised from the 1-dimensional quantum kicked rotor by temporally varying the kicking strength with incommensurate frequencies [8]. The kicking strength is varied as :

$$\tilde{\kappa} = \kappa(t) = \kappa_0(1 + \epsilon\cos(\omega_2 t + \phi_2)\cos(\omega_3 t + \phi_3)) \tag{13}$$

while $\hat{\mathcal{H}}_{\tilde{\kappa}} = p^2/2 + \tilde{\kappa}\cos(x)\delta_\tau(t)$. Such a quasi-periodic kicked rotor (QPKR) is numerically easier to simulate since it requires only one spatial dimension, but displays all properties of 3D systems. In the previous section, we derived the equivalence relation between the QKR and a CTQW. Here, we develop a relation between the QPKR at resonance and the CTQW by temporally varying the transition probability, $\gamma(t)$.
Consider a series of time-modulated kicks $(\kappa_1, \kappa_2, ...\kappa_{T-1})$ supplied to a QKR at resonance until time T. Such a QKR exhibits the dynamics of a QPKR and condition(12) is satisfied between two consecutive kicks. Then the total unitary operator till an integer timestep T for the QKR is given by:

$$\begin{aligned}
\mathcal{U}(T) &= \mathcal{U}(T-1)\mathcal{U}(T-2)...\mathcal{U}(1) \\
&= \exp(-i\mathcal{H}_{\tilde{\kappa}}(T-1))\exp(-i\mathcal{H}_{\tilde{\kappa}}(T-2))...\exp(-i\mathcal{H}_{\tilde{\kappa}}(1)) \\
&= \exp(-2i\gamma(T-1)\mathcal{I} - i\mathcal{H}_{\tilde{\gamma}}(T-1))\exp(-2i\gamma(T-2)\mathcal{I} - i\mathcal{H}_{\tilde{\gamma}}(T-2))...\exp(-2i\gamma(1)\mathcal{I} - i\mathcal{H}_{\tilde{\gamma}}(1)) \\
&= \left(\Pi_{l=1}^{T}\exp(-2i\tilde{\gamma}(l)\mathcal{I})\right)\left(\Pi_{t=1}^{T}\exp(-i\mathcal{H}_{\tilde{\gamma}}(t))\right) \\
&= \exp\left\{-2i(\sum_{t=1}^{T-1}\tilde{\gamma}(t))I\right\}\exp\left\{i\sum_{t=1}^{T-1}\mathcal{H}_{\tilde{\gamma}}(t)\right\} \\
&= \exp\left\{-2i\Gamma\mathcal{I}\right\}\exp\left\{i\widetilde{\mathcal{H}}_{\tilde{\gamma}}\right\} = \exp\left\{-i(2\Gamma\mathcal{I} - \widetilde{\mathcal{H}}_{\tilde{\gamma}})\right\}
\end{aligned}$$

Thus, under the condition of $2\tilde{\gamma} = \tilde{\kappa}$, the dynamics of a QPKR at resonance can be realised by sinusoidally varying the transition probabilities of a CTQW given by the QKR hamiltonian in momentum space.

7 Quantum state preparation with QKR-CTQW

The probability distributions after some time-evolutions of the QKR at resonance conditions, or equivalently of a CTQW on the line, show interesting interference patterns, which can be controlled by the relative phases in the initial states. This allows us to realize various kinds of final distributions based on initial configurations in the walker's space. In fig(6), we show how the probability distribution changes by choosing different values for the respective coefficients.

Since the symmetry of the delta-function initial state is broken, the parity properties of the Bessel functions suppress the two external peaks. This leads to a strong interference of the participating momentum states. In general, the CTQW, or the equivalent QKR evolution at resonance, can be steered, biased towards one direction, and be made more localized or broader depending only on the specific choice of the initial state.
Consider the initial state:

$$\psi_0(\bar{C}) = \frac{1}{3}\frac{1}{\sqrt{2\pi}}(C_{-1}|-1\rangle + C_0|0\rangle + C_1|1\rangle)$$

$$\langle p|\psi_0(\bar{C})\rangle = \frac{1}{3}\frac{1}{\sqrt{2\pi}}(C_{-1}e^{-i\theta} + C_0 + C_1e^{i\theta}) \tag{14}$$

We consider a thermal distribution over three states with all coefficients chosen to be modulus equal to one ie $C_j = e^{i\phi_j}$ while setting $C_0 = 1$ by the choice of the global phase.

$$\begin{aligned} P_1 &= J_n^2(2\gamma t) + J_{n1}^2(2\gamma t) + J_{n+1}^2(2\gamma t) \\ P_2 &= Im[C_0C_1]J_n(2\gamma t)J_{n1}(2\gamma t) \\ P_3 &= Im[C_0C_1]J_n(2\gamma t)J_{n+1}(2\gamma t) \\ P_4 &= Re[C_1C_1]J_{n1}(2\gamma t)J_{n+1}(2\gamma t) \\ P_{(\gamma,\bar{C})}(n,t) &= \frac{1}{3}(P_1 + 2P_2 - 2P_3 - 2P_4) \end{aligned} \tag{15}$$

where$P_{(\gamma,\bar{C})}(n,t)$ represents the probability of finding the walker at state 'n' at time 't'. Delvecchio et al show how the coefficients in the initial state can be optimized in order to obtain a target distribution after a given number t of kicks [9]. In particular, any target distribution over N basis states can be realised, given that a generic superposition of only a few states can be experimentally realized as the input state. The obtained distributions are of particular relevance for realizing a quantum search protocol. The initial state $\mathcal{C}$ for such a distribution can be obtained by minimizing the difference between the time-evolved distribution of the QKR at resonance and the desired target distribution. The maximal width after t kicks can be estimated to be $N \approx \pi\kappa t$ and the final distribution can directly be engineered given the choice of the initial coefficients, the coupling parameter $\kappa(2\gamma)$, and the number of evolution steps.

8 Detection time for a QKR-CTQW

The distribution of first arrival times or hitting times of a classical random walker was first characterized by Schrodinger through the renewal equation that relates the probability of the first arrival at a site and the occupation probabilities [10]. For the simple case of an unbiased random

walker on a 1D lattice, the first-passage time follows a Lévy distribution, decaying like $t^{-\frac{3}{2}}$, and has immense applications in varied fields like electronics, financial modeling, etc [11–13]. Contrary to classical random walks, quantum walks (under certain conditions) can provide a quadratic speedup, and investigating the first arrival times for such walks is paramount to characterize the running times of quantum search algorithms. Further, recent advances in experimental atom-optics, single-particle quantum tracking, and measurement have made it possible to realize quantum walks with larger coherence times and higher dimensionality [14].

To discuss the first-arrival times in quantum walks, we need to distinguish between arrival vs detection times. Even in the classical case, the two times are different since the time of the first detection does not imply that the particle first arrived at the site if the sampling was not continuous. In the quantum case, the postulate of unitary evolution forbids any random motion while projective measurements necessitate the collapse of the wavefunction post-measurement. Since we cannot obtain the trajectory of a quantum particle, the problem of arrival times becomes ill-defined. Therefore, we treat the problem of first detection times under repeated stroboscopic measurements. In the following sections, we derive the recently proposed quantum-renewal equation to obtain the statistics of first detection times[15, 16] and apply it to the quantum-kicked rotor system at resonance.

Measurement protocol
Consider a particle that performs a CTQW governed by the hamiltonian in equation.10 on a line graph (like a tight-binding model). Our goal is to detect the wave function at a site of interest, say 'x' by performing stroboscopic measurements at a sampling rate of τ.
We start with an initial wavefunction $|\psi(0)\rangle$ and evolve it until time τ. Then, the detection of the particle at the target site is attempted, and with probability P_1 the first measurement is also the first detection. Computationally, there are two ways to simulate such a procedure: either consider a fixed threshold probability of detection or consider a uniform random number between $(0, 1)$ and compare this with the detected probability. The former relies on the fact that the detector samples continuously with a fixed accuracy and is only used to probe the system at the sampling times $(n\tau)$ while the latter models a more general case. If the particle is detected, the measurement time is τ. If the particle is not detected, we compute P_2 using the quantum renewal equation (12.4). Then, at time 2τ either the particle is detected with probability P_2 or not. Thus, the probability of measuring the particle for the first time after n = 2 attempts is $F_2 = (1 - P_1)P_2$. This process is repeated until a measurement is recorded, and such a measurement is logged as the random first detection event. To construct the first detection probability, we initialize an ensemble of such particles and apply the described procedure.

8.1 Fixed detection threshold

Here, we fix a detection threshold (ϵ_D), and consider the particle to be detected at n such that $p_x(\bar{c}, n\tau) \geq \epsilon_D$ where $\bar{C}$ is the initial wave-function as described in equation.14, x is the detection site, τ is the sampling time, and ϵ_D is the detection threshold (characteristic of the detection device and calibration technique). We sample over different initial states since under unitary evolution, a fixed initial condition and detection threshold, always yield the same detection time. We consider a thermal state $\psi(0) \sim [0 \ldots C_{-1}, 1, C_1, \ldots]$ such that $|C_{-1}|^2 = |C_1|^2 = 1$. Each C_i can be given by $e^{i\phi}$ where $\phi \approx U(0, 2\pi)$. We thus obtain a distribution of detection times for QKR-CTQW over different initial conditions due to the interference of the competing waves from the initial conditions. [Fig 7]

8.2 Threshold independent detection

The purpose of a threshold for detection probability can be justified by the knowledge of the exact measurement technique employed. However, a more general threshold-independent detection can be performed by sampling from a uniform distribution between (0,1) and comparing this value with the detected probability P_n ie we want $\{n|p_k(n\tau) > U(0,1)\}$ using the quantum renewal equation[20,21]. Such a process mimics the desired probabilities of $F_n = (1-P_1)(1-P_2)..P_n$ since the probability of detection of being more than P_1 is equal to the probability of obtaining more than P_1 from a $U(0,1)$ sampling. In Fig 8, we plot a few results from simulating a threshold-independent detection process for a quantum-kicked rotor at resonance. We observe a n^{-3} decay when the detection is performed at the target site $|0\rangle$.

8.2.1 Detection times in the presence of noise

Quantum walks can be steered to obtain a desired average momentum distribution by sampling the kicking strengths from a narrow distribution with Bose-Einstein condensates [17]. In Fig 9, we plot at distribution of detection times when the kicking strengths for the kicked rotor is sampled from a narrow gaussian distribution as a proxy for small detunings from quantum resonance.

9 Conclusions and Outlook

We have studied the quantum resonance phenomena in periodically-kicked quantum rotor systems and how such a system can be mapped to a continuous-time quantum walk model in momentum space. Using the scheme proposed in section 7, such a mapping is useful to dynamically engineer initial states to obtain desired target distributions through unitary evolutions. When the initial state violates parity symmetry, a ratchet effect can be seen where the walk is directed towards one direction and suppressed in the other. The parameter space plots like Fig**??** can be used to

prepare thermal states and choose kicking strengths to optimize the detection times at a desired state. Furthermore, we characterize the condition for quantum advantage in searching for encoded momentum states using the first detection-time distribution (FDTD). However, such an advantage is suppressed or lost when the kicks delivered to the rotor are drawn from a narrow gaussian distribution.

Future work can be focussed in two specific directions. The first involves the investigation of the behaviour of the FDTD, for example, at long timescales does the noisy kicked-QKR at resonance display similar behaviour with classical walks? How does the FDTD behave for a time-dependent kicking strength? What happens to the FDTD when initial states violate parity? Are their any universal features? The second direction would be two use the QKR-CTQW as a tool for quantum computing taks. Since discrete-time quantum walks are a model for universal quantum computation, can we augment the CTQW-QKR-at resonance with a coin-space where the phase of state $|0\rangle$ can be flipped as a coin at discrete times? The dynamics and entanglement features of manybody-kicked rotors can be studied. In the context of searching for states, can we learn the sequence of unitaries to be applied to the QKR-at-resonance to obtain a desired average momentum state? How should we choose the initial state that breaks parity symmetry for such a task? We feel that these questions can be addressed within the interdisciplinary fields of quantum computing, quantum chaos and machine learning.

10 Acknowledgment

The idea of studying the relationship between quantum walks and quantum kicked rotors at resonance was suggested by my supervisor Prof MS Santhanam. I would like to thank him for his continued patience, support and guidance during the entire semester. I would like to thank J.Bharathi Kannan for many invaluable discussions, and Aanjaneya Kumar for his insights on analysing hitting times of random walks, paper recommendations, and allowing me to use his system for running lengthy simulations. I would like to thank the institute and the entire department of physics for the support I have been offered.

11 References

References

[1] MS Santhanam, Sanku Paul, and J Bharathi Kannan. Quantum kicked rotor and its variants: Chaos, localization and beyond. *Physics Reports*, 956:1–87, 2022.

[2] Boris Valerianovich Chirikov. Research concerning the theory of non-linear resonance and stochasticity. Technical report, CM-P00100691, 1971.

[3] AK Sikri and ML Narchal. Floquet states of a periodically kicked particle. *Pramana*, 40(4):267–272, 1993.

[4] Shmuel Fishman, DR Grempel, and RE Prange. Chaos, quantum recurrences, and anderson localization. *Physical Review Letters*, 49(8):509, 1982.

[5] Eyal Doron and Shmuel Fishman. Anderson localization for a two-dimensional rotor. *Physical review letters*, 60(10):867, 1988.

[6] FM Izrailev and Dmitrii L'vovich Shepelyanskii. Quantum resonance for the rotor in a nonlinear periodic field. In *Doklady Akademii Nauk*, volume 249, pages 1103–1107. Russian Academy of Sciences, 1979.

[7] Yakir Aharonov, Luiz Davidovich, and Nicim Zagury. Quantum random walks. *Physical Review A*, 48(2):1687, 1993.

[8] Jiao Wang and Antonio M Garcia-Garcia. Anderson transition in a three-dimensional kicked rotor. *Physical Review E*, 79(3):036206, 2009.

[9] Michele Delvecchio, Francesco Petiziol, and Sandro Wimberger. Resonant quantum kicked rotor as a continuous-time quantum walk. *Condensed Matter*, 5(1):4, 2020.

[10] Erwin Schrödinger. Zur theorie der fall-und steigversuche an teilchen mit brownscher bewegung. *Physikalische Zeitschrift*, 16:289–295, 1915.

[11] Sidney Redner et al. *A guide to first-passage processes*. Cambridge university press, 2001.

[12] Vadim Linetsky. Lookback options and diffusion hitting times: A spectral expansion approach. *Finance and Stochastics*, 8(3):373–398, 2004.

[13] George A Whitmore. First-passage-time models for duration data: regression structures and competing risks. *Journal of the Royal Statistical Society: Series D (The Statistician)*, 35(2):207–219, 1986.

[14] Siamak Dadras, Alexander Gresch, Caspar Groiseau, Sandro Wimberger, and Gil S Summy. Quantum walk in momentum space with a bose-einstein condensate. *Physical review letters*, 121(7):070402, 2018.

[15] Shrabanti Dhar, Subinay Dasgupta, Abhishek Dhar, and Diptiman Sen. Detection of a quantum particle on a lattice under repeated projective measurements. *Physical Review A*, 91(6):062115, 2015.

[16] H Friedman, DA Kessler, and E Barkai. Quantum renewal equation for the first detection time of a quantum walk. *Journal of Physics A: Mathematical and Theoretical*, 50(4):04LT01, 2016.

[17] Marcel Weiß, Caspar Groiseau, WK Lam, Raffaella Burioni, Alessandro Vezzani, Gil S Summy, and Sandro Wimberger. Steering random walks with kicked ultracold atoms. *Physical Review A*, 92(3):033606, 2015.

[18] Renato Portugal. *Quantum walks and search algorithms*, volume 19. Springer, 2013.

[19] Felix Thiel, Eli Barkai, and David A Kessler. First detected arrival of a quantum walker on an infinite line. *Physical review letters*, 120(4):040502, 2018.

12 Appendix

12.1 Chirikov map for classical rotor

The non-dimensionalised form of the classical rotor is : $H(p,q,t) = p^2/2 - \kappa\cos(q)\delta_1(t)$. Using Hamilton's equations of motion we get: (1) $\dot{p} = -\partial_q\mathcal{H} = -\kappa(q)\delta_1(t)$ and $\dot{q} = \partial_p\mathcal{H} = p$. Now we integrate both these equations between two successive kicks: (τ_n, τ_{n+1}).

$$\lim_{\beta\to 0}\int_{\tau_n-\beta}^{\tau_{n+1}-\beta} dp = -\lim_{\beta\to 0}\kappa\sin q\int_{\tau_n-\beta}^{\tau_{n+1}-\beta}\delta_1(t)dt$$

$$\lim_{\beta\to 0}[p(\tau_{n+1}-\beta) - p(\tau_n-\beta)] = -\kappa\sin q$$

using $\beta \to 0$, we get:

$$p(\tau_{n+1}) - p(\tau_n) = -\kappa\sin(q)$$

Now we integrate q between successive kick timings:

$$\lim_{\beta\to 0}\int_{\tau_n-\beta}^{\tau_{n+1}-\beta} dq = \lim_{\beta\to 0}\int_{\tau_n-\beta}^{\tau_{n+1}-\beta} pdt$$

$$\lim_{\beta\to 0}[q(\tau_{n+1}-\beta) - q(\tau_n-\beta)] = \lim_{\beta\to 0}[p(\tau_{n+1}-\beta)(\tau_{n+1}-\beta) - p(\tau_n-\beta)(\tau_n-\beta)]$$

(We use the fact that between two kicks, momentum is conserved.)

$$q(\tau_{n+1}) - q(\tau_n) = \tau_{n+1}p(\tau_{n+1}) - \tau_n p(\tau_n) = p(\tau_{n+1})$$

Combining both the results, we obtain the Chirikov map:

$$p_{n+1} = p_n + \kappa\sin(q_n) \tag{16}$$

$$q_{n+1} = q_n + p_{n+1} \tag{17}$$

To find the general expression for $\langle(\Delta p)^2\rangle$: From the standard map, we know that $p(n) = p(0) + \kappa\sum_{i=0}^{n}\sin_{x_i}$. Then:

$$\begin{aligned}\langle(\Delta p)^2\rangle &= \langle(p(n)-p(0))^2\rangle \\ &= \kappa^2(\sum_{i=0}^{n-1}\langle\sin^2(x_i)\rangle + \sum_{i\neq j}\langle\sin(x_i)\sin(x_j)\rangle\end{aligned}$$

The first average on the RHS evaluates to 1/2 while the second average is equal to 0. Thus we obtain the diffusive behaviour relation: $\langle(\Delta p)^2\rangle = \frac{1}{2}\kappa^2 n$

12.2 Generator of Transition Matrix

Let $\mathcal{M}$ be the stochastic matrix for a continuous time random walk. Due to the property of markovity, a time-evolution of ϵ can be decomposed into:

$$\begin{aligned}\mathcal{M}_{ij}(t+\epsilon) &= \sum_k \mathcal{M}_{ik}(t)\mathcal{M}_{kj}(\epsilon) \\ &= \mathcal{M}_{ij}(t)\mathcal{M}_{jj}(\epsilon) + \sum_{k\neq j}\mathcal{M}_{ik}(t)\mathcal{M}_{kj}(\epsilon) \\ &= \mathcal{M}_{ij}(t)[1-\mathcal{H}_{jj}] + \sum_{k\neq j}\mathcal{M}_{ik}(t)\mathcal{H}_{kj}(t) \\ \frac{1}{\epsilon}\left(\mathcal{M}_{ij}(t+\epsilon)-\mathcal{M}_{ij}(t)\right) &= -\mathcal{H}_{jj} + \frac{1}{\epsilon}\sum_{k\neq j}\mathcal{M}_{ik}(t)H_{kj} \\ \lim_{\epsilon\to 0}\frac{d\mathcal{M}_{ij}(t)}{dt} &= -\sum_k \mathcal{H}_{kj}\mathcal{M}_{ik}(t)\end{aligned}$$

Thus, we can write $\mathcal{M} = e^{-\mathcal{H}t}$

12.3 Calculations for the Distributions of CTQW

In this section we calculate explicitly the distribution of the CTQW for the system initialized in the zero momentum state $|0\rangle$. As an exercise, we leave it to the reader to verify the following by mathematical induction:

$$\bar{\mathcal{H}}_\gamma^t|0\rangle = \gamma^t\sum_{n=-t}^{t}(-1)^n\binom{2t}{t-n}|n\rangle$$

Our aim is to compute $\mathcal{U}(t)|0\rangle$. We begin by expanding the operator as:

$$\mathcal{U}(t)|0\rangle = e^{-i\bar{\mathcal{H}}_\gamma t} = \sum_{k=0}^{\infty} \frac{(-i\bar{\mathcal{H}}_\gamma t)^k}{k!} = \sum_{k=0}^{\infty} \frac{(-it)^k}{k!} \left(\gamma^k \sum_{n=-k}^{k} (-1)^n \binom{2k}{k-n} |n\rangle \right)$$

This can be solved by interchanging the summation orders are rewriting as:

$$\begin{aligned} \mathcal{U}(t)|0\rangle &= \sum_{n=-\infty}^{\infty} \sum_{k=|n|}^{\infty} \frac{(-i\gamma t)^k}{k!} (-1)^{|n|} \binom{2k}{k-n} |n\rangle \\ &= \sum_{n=-\infty}^{\infty} \exp(i\frac{\pi}{2}|n|) \exp(i\frac{\pi}{2}|n|) \sum_{k=|n|}^{\infty} \frac{(-i\gamma t)^k}{k!} (-1)^{|n|} \binom{2k}{k-n} |n\rangle \end{aligned}$$

We now use the Bessel function identity:

$$\exp(-2i\gamma t) J_{|n|}(2\gamma t) = \exp(i\frac{\pi}{2}|n|) \sum_{k=|n|}^{\infty} \frac{(-i\gamma t)^k}{k!} (-1)^{|}n| \binom{2k}{k-n}$$

$$\text{we obtain: } \mathcal{U}(t)|0\rangle = \sum_{n=-\infty}^{\infty} \exp(i\frac{\pi}{2}|n| - 2i\gamma t) J_{|n|}(2\gamma t)|n\rangle$$

From this expression, we can evaluate the probability distribution at a general time 't' as :

$$P_\gamma(n,t) = |\langle n|\mathcal{U}(t)|0\rangle|^2 = |J_n(2\gamma t)|^2$$

12.3.1 Initial states for obtaining distributions

We have used the following initial states to obtain the distributions in Fig**??**. We work with a basis size of 256x256. The unitary matrix is obtained using equation7. Each C_i is the values of the initial state phase described in equation14.

$C_1 = [1]$ $C_2 = [1, 1, -1]$ $C_3 = [1j, 1, -1j]$
$C_4 = [1j, 1, 1j]$ $C_5 = [\exp(-i\pi/5), 1, \exp(-i\pi/5)])$ $C_6 = [1, 1, 1, -1, 1]$
$C_7 = [0.40, 0.75, 0.52, 0.06]$ $C_8 = [0.23, 0.67, 0.67, 0.23]$ $C_9 = [0.48, 0.73, 0.48]$

12.4 Quantum renewal equation

In this section, we investigate the probability of detecting a quantum particle undergoing a continuous time quantum walk according to equation 10. We perform stroboscopic measurements

at the target site 'x' at discrete times: $\{\tau, 2\tau, ...n\tau\}$ until the detector records the particle. The measurement provides two possible outcomes: either the particle is at the target site or not. Initialy, the system is prepared in a state $|\psi(0)\rangle$. Consider the first measurement, at time τ. At $\tau^- = \tau - \epsilon$ with $\epsilon \to 0$ being positive, the wave function is $|\psi(\tau^-\rangle = \mathcal{U}(\tau)|\psi(0)\rangle$ where $\mathcal{U} = \exp(-i\mathcal{H}t/\hbar)$. Putting $\hbar = 1$, the probability of finding the particle at 'x' is given by: $P_1 = |\langle x|\psi(\tau^-)\rangle|^2$. If the measurement is positive, then the particle is said to be found at 'x', and the first detection time (FDT) is $t_f = \tau$. If the particle is not detected (occurs with probability $1 - P_1$), then the quantum system is evolved for another sampling time τ. Post this measurement, the state of the system is $|\psi(\tau^+)\rangle = (1-|x\rangle\langle x|)/(\sqrt{1-P_1})|\psi(\tau^-)\rangle$. In essensce, the measurement nullifies the wave functions on 'x' and maintains the relative amplitudes of finding the particles outside the spatial domain of measurement device. Now, just before the time of second measurement, the state of the system is: $\psi(2\tau^-) = \mathcal{U}(\tau)|\psi(\tau^+)\rangle$. The probability of finding the particle at 'x', given that the first measurement returned null is: $P_2 = |\langle x|\mathcal{U}(\tau)|\psi(\tau^+)\rangle|^2$.
To obtain a more general expression, we define the projection operator, $\hat{D} = |x\rangle\langle x|$. This enables us to write : $P_2 = \frac{|\langle x|\mathcal{U}(\tau)(1-\hat{D})\mathcal{U}(\tau))|\psi(0)\rangle|^2}{1-P_1}$. This iteration can be continued to obtain the expression:

$$P_n = \frac{|\langle x|[\mathcal{U}(\tau)(1-\hat{D})]^{n-1}\mathcal{U}(\tau)|\psi(0)\rangle|^2}{\Pi_{i=1}^{n-1}(1-P_i)} \tag{18}$$

We define the first detection wave function as:

$$|\theta_n\rangle = \mathcal{U}(\tau)[1-\hat{D}\mathcal{U}(\tau)]^{n-1}|\psi(0)\rangle \tag{19}$$

or $\theta_n\rangle = \mathcal{U}(\tau)[1-\hat{D}]^{n-1}|\theta_1$. This leads us to a general expression for P_n, the probability of first detection at the 'n' measurement, given the first 'n-1' measurements as null.

$$P_n = \frac{\langle\theta_n|\hat{D}|\theta_n\rangle}{\Pi_{j=1}^{n-1}(1-P_j)} \tag{20}$$

To simulate this process, we sample a uniform random number between (0,1) and compare it with P_1, if the particle is detected, the measurement time is τ . If the particle is not detected, we compute P_2. We perform the procedure again to comapre a random number from U(0,1) with P_2, if P_2 is larger, the first detection time is 2τ. The probability of measuring the particle for the first time after n = η attempts is then : $F_\eta = (1-P_1)(1-P_2)...P_\eta = \langle\theta_\eta|\hat{D}|\theta_\eta\rangle$.
We define the amplitude of first detection as $\phi_n = \langle x|\theta_n$ such that $F_n = |\phi_n|^2$. Using the expression for θ_n, we get: $\phi_1 = \langle x|\mathcal{U}(\tau)|\psi(0)\rangle$, $\phi_2 = \langle x|\mathcal{U}(\tau)|\psi(0) - \phi_1\langle x|\mathcal{U}(2\tau)|x\rangle$, and by induction we obtain, our main result, the quantum renewal equation.:

$$\phi_n = \langle 0|\mathcal{U}(n\tau)|\psi(0) - \sum_{j=1}^{n-1}\phi_j\langle 0|\mathcal{U}[n-j]\tau]|x\rangle \tag{21}$$

ϕ_n is the amplitude for being at site 'x' at time $n\tau$ in the absence of measurements, from which we subtract $n-1$ terms related to the previous history of the system. The intuitive idea is that the condition of non-detection in previous measurements translates into subtracting wave sources at the detection site $|x\rangle$ following the j^{th} detection attempt. The evolution of that wave source from the j^{th} measurement onwards is described by the free Hamiltonian, hence, $\langle x|U[(n-j)\tau]|x\rangle$ which yields the amplitude of first detection at 'x' in the time interval $(j\tau, n\tau)$.

13 Figures

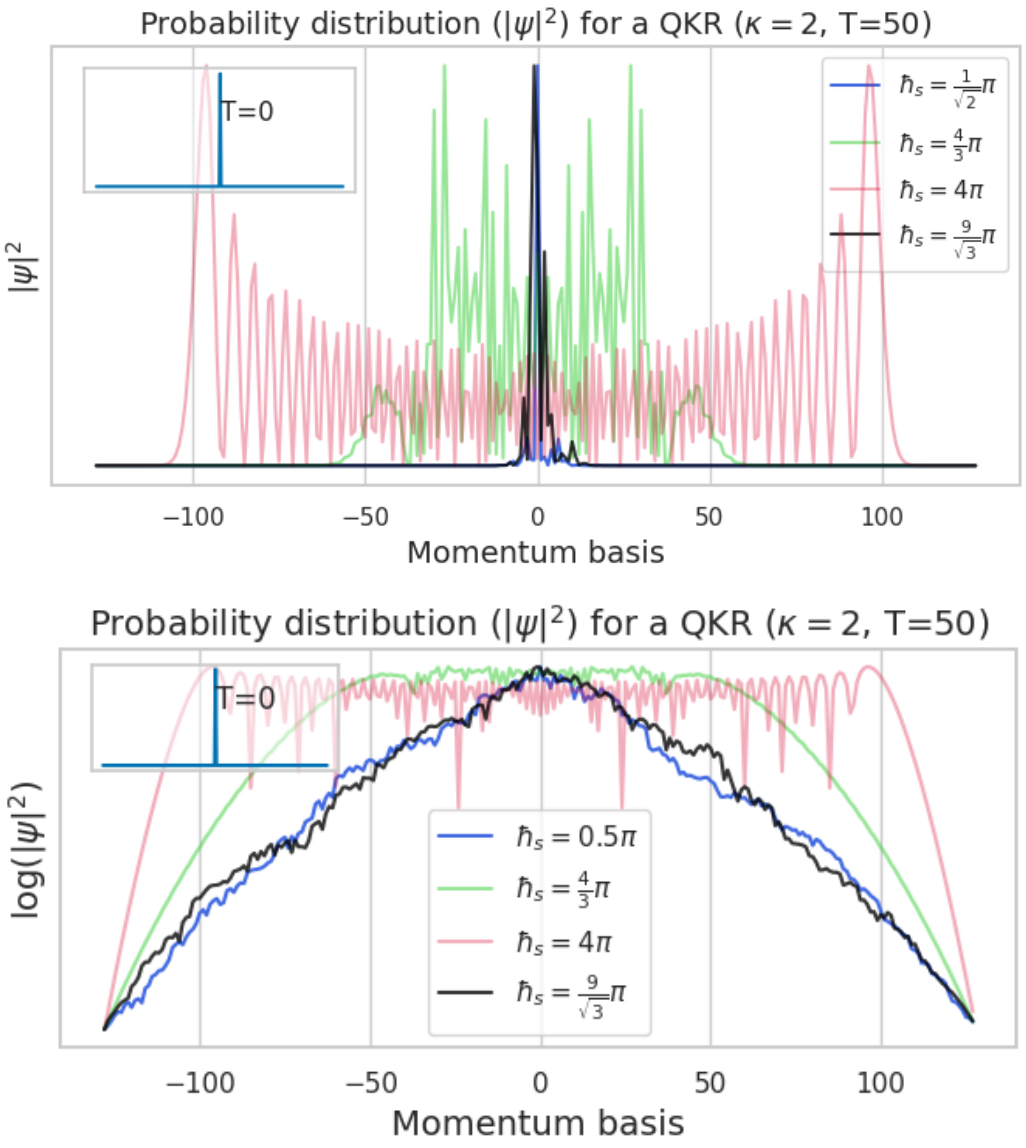

Figure 1: Evolution of the Quantum kicked rotor for different $\hbar_s$. When $\hbar_s$ is an integral multiple of 4π, quantum resonance is observed and the initial state $|0\rangle$ spreads ballistically. For incommensurate values of $\hbar_s/4\pi$, we observe dynamical localisation of states.

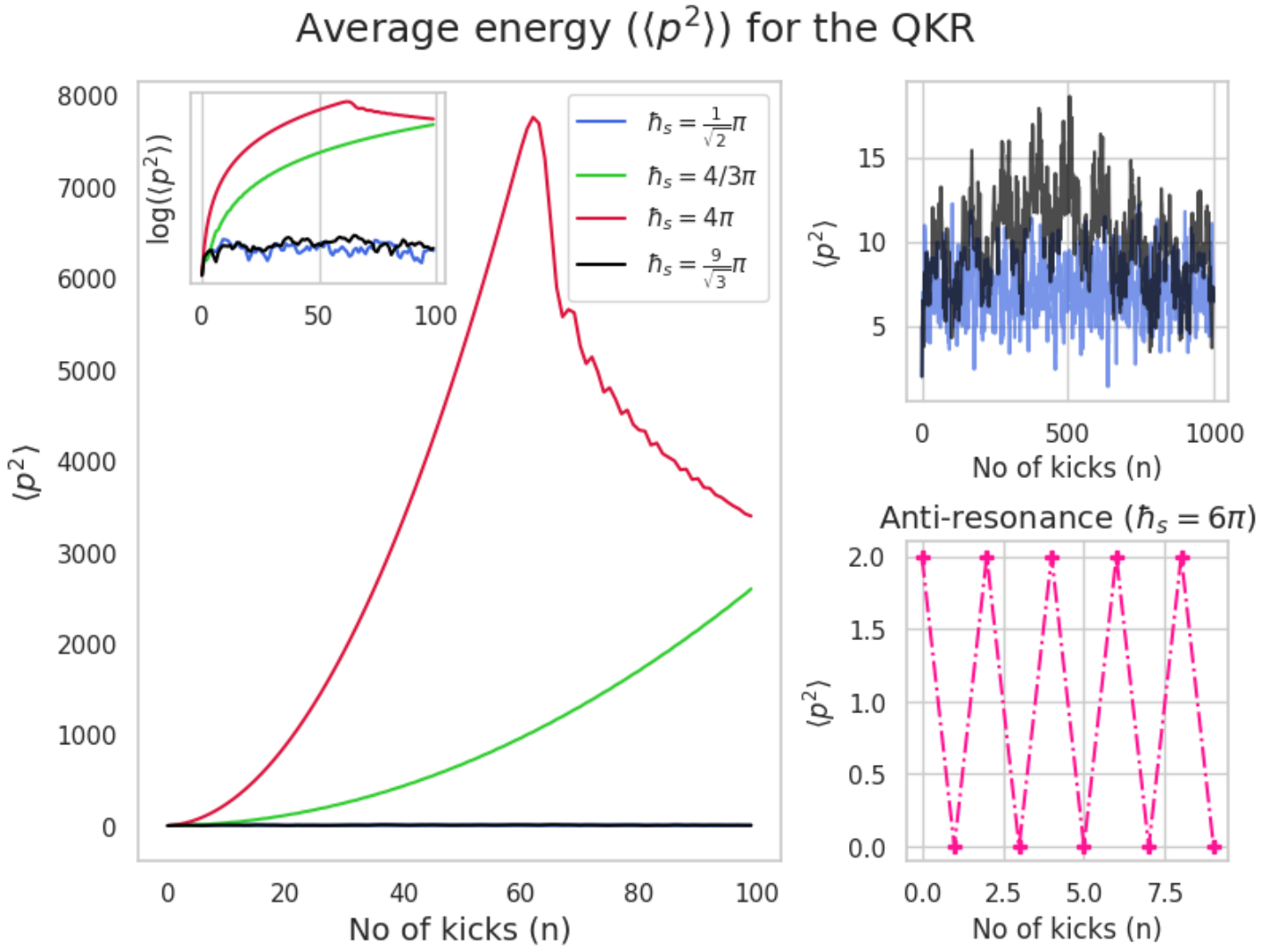

Figure 2: Dynamics of Quantum kicked rotor at resonance. At resonance, the floquet spectrum is continuous and this leads to a quadratic growth in average energy of the system $\langle E \rangle$. For incommensurate $\hbar/4\pi$, the average energy saturates due to localization. For the case of anti-resonance, the average energy oscillates between two values since successive evolutions yield the initial state.

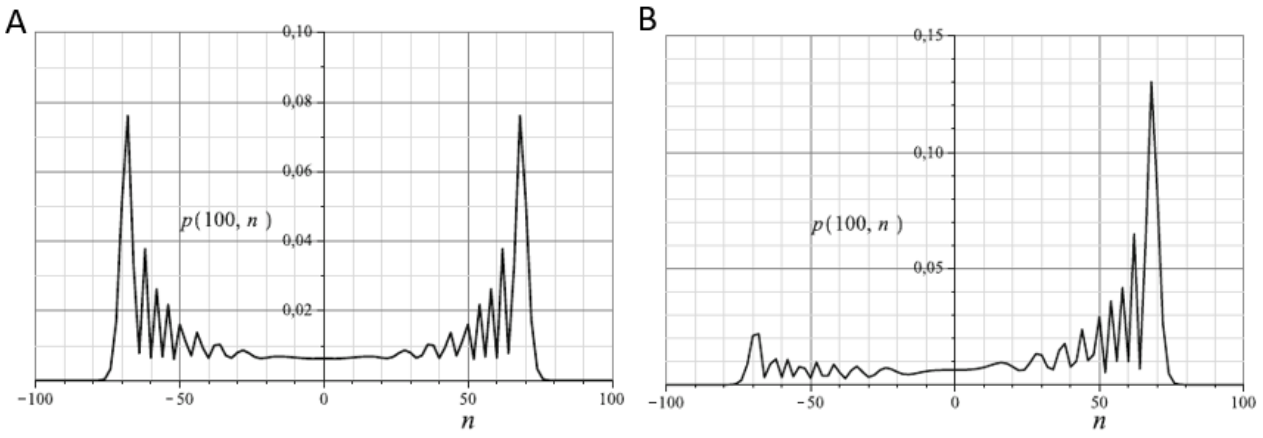

Figure 3: Left:Probability distribution after 100 steps of a quantum walk with the Hadamard coin starting from the initial condition: $\psi(0)\rangle = (2/\sqrt{2})(|0\rangle - i|1)|n = 0\rangle$. Right: Probability distribution after 100 steps of a quantum walk with the Hadamard coin starting from the initial condition $|\psi(0)\rangle = |0\rangle$. (Source: [18])

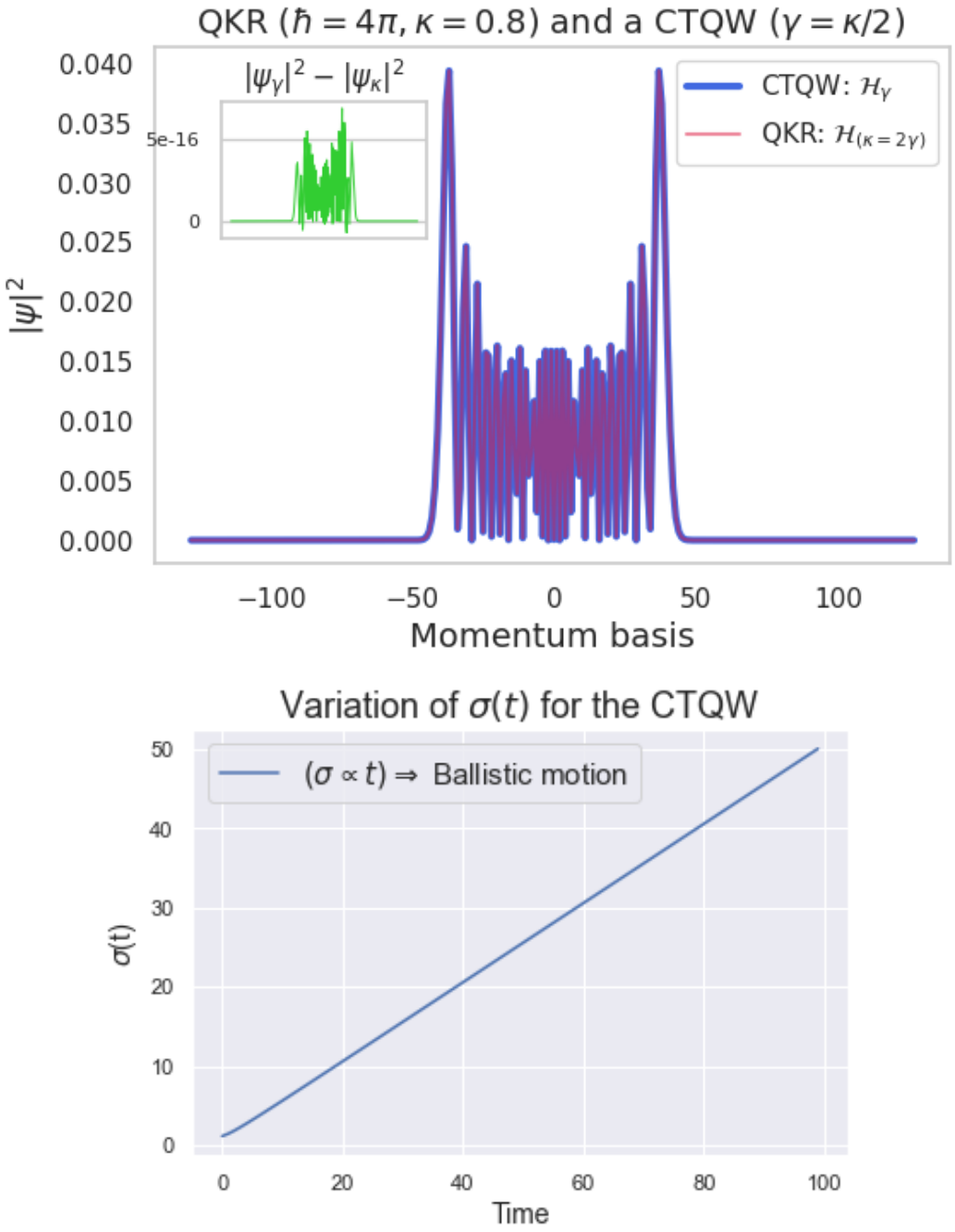

Figure 4: Top: The probability distributions of the CTQW and the QKR at resonance. For $\kappa = 2\gamma$ and $\hbar_s = 4\pi$, both systems follow the same dynamics and the resultant probability distributions superpose. Bottom: The standard deviation in a CTQW is $\propto t$ indicative of ballistic motion.

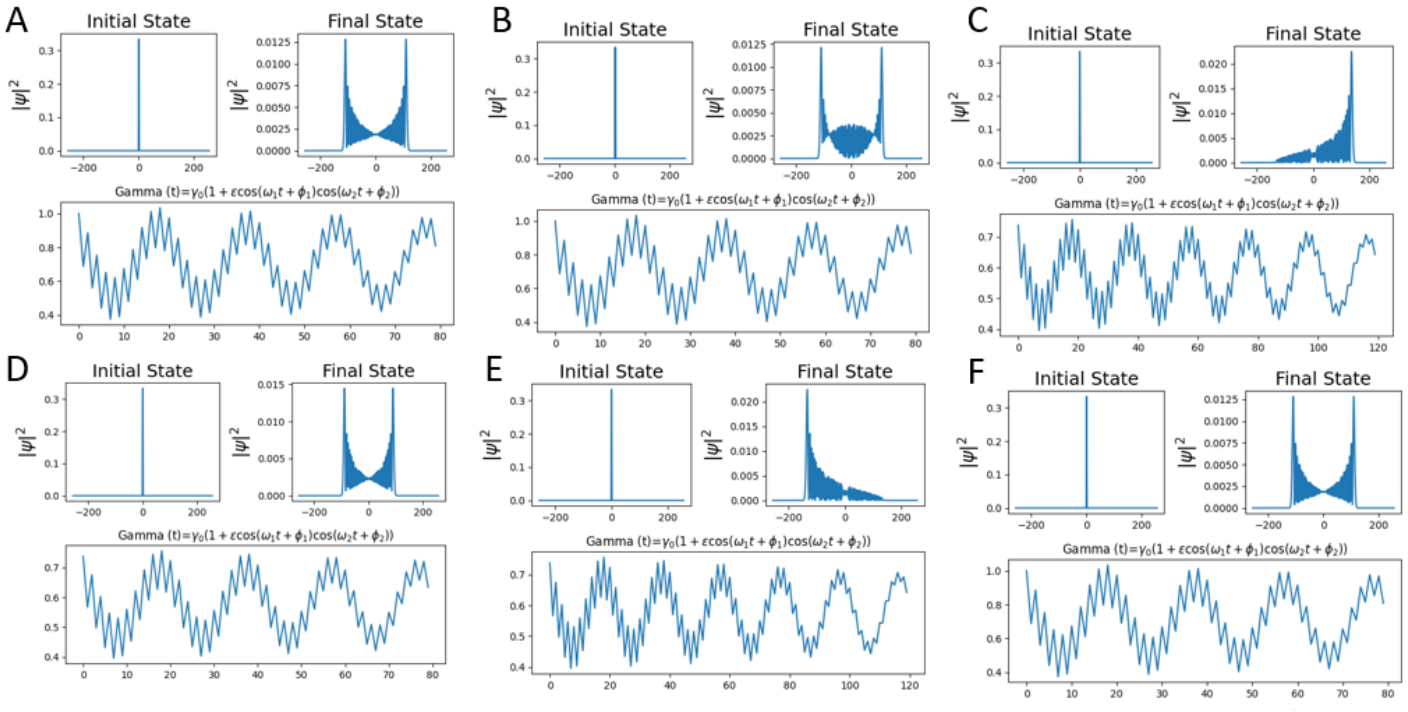

Figure 5: Time-dependent QKR-CTQW. Here the kicking strength $\kappa = 2\gamma$ is time-dependent and given by eq13. By choosing the optimum values of ϵ, γ_0, almost any target distribution can be realised. The dynamics can is analogous to the quasiperiodic kicked rotor system.

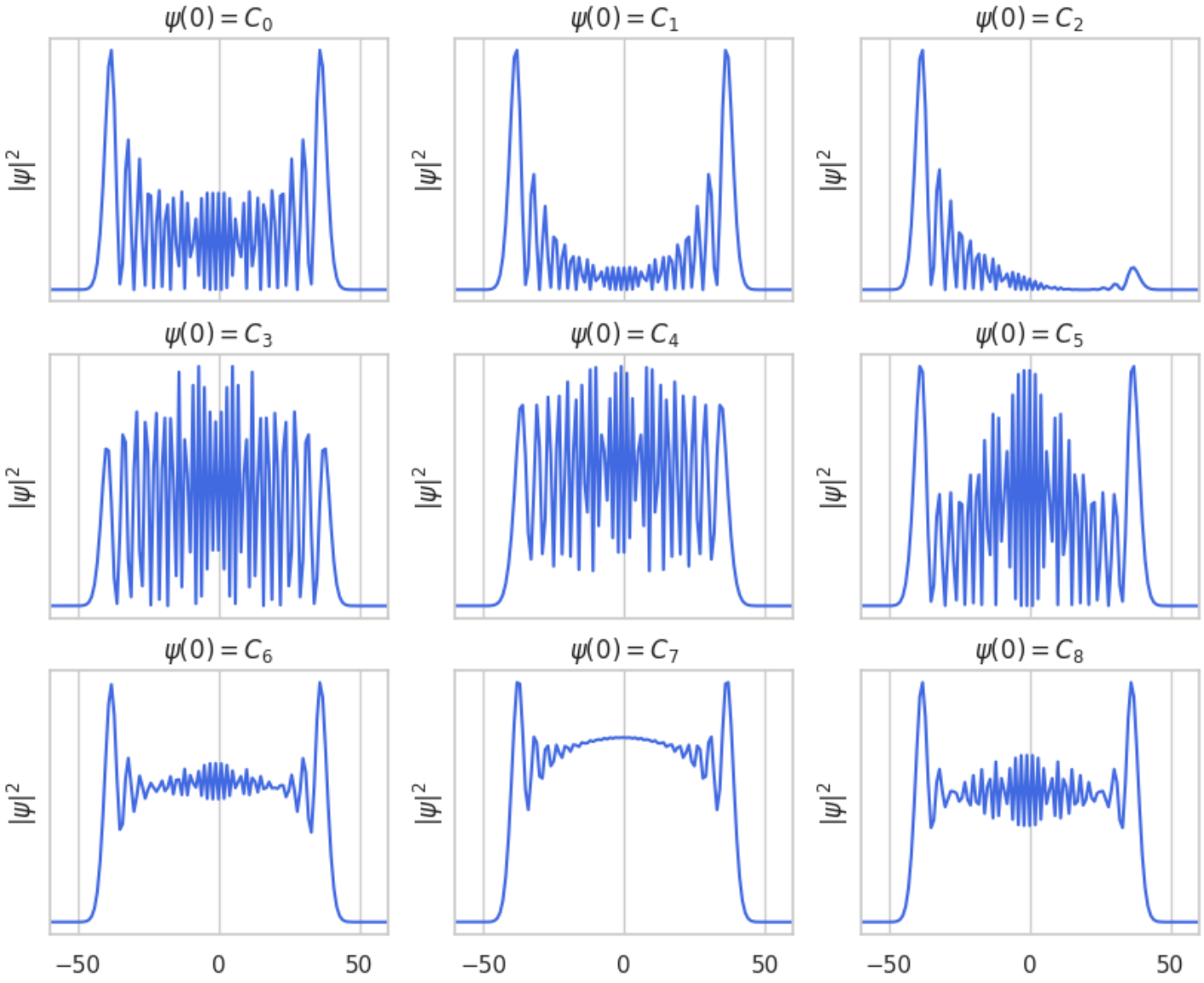

Figure 6: Quantum state preparation with QKR-CTQW. Using different initial conditions, the desired target distribution can be obtained after certain unitary evolutions. Values of each C_i is mentioned in Appendix(12.3.1)

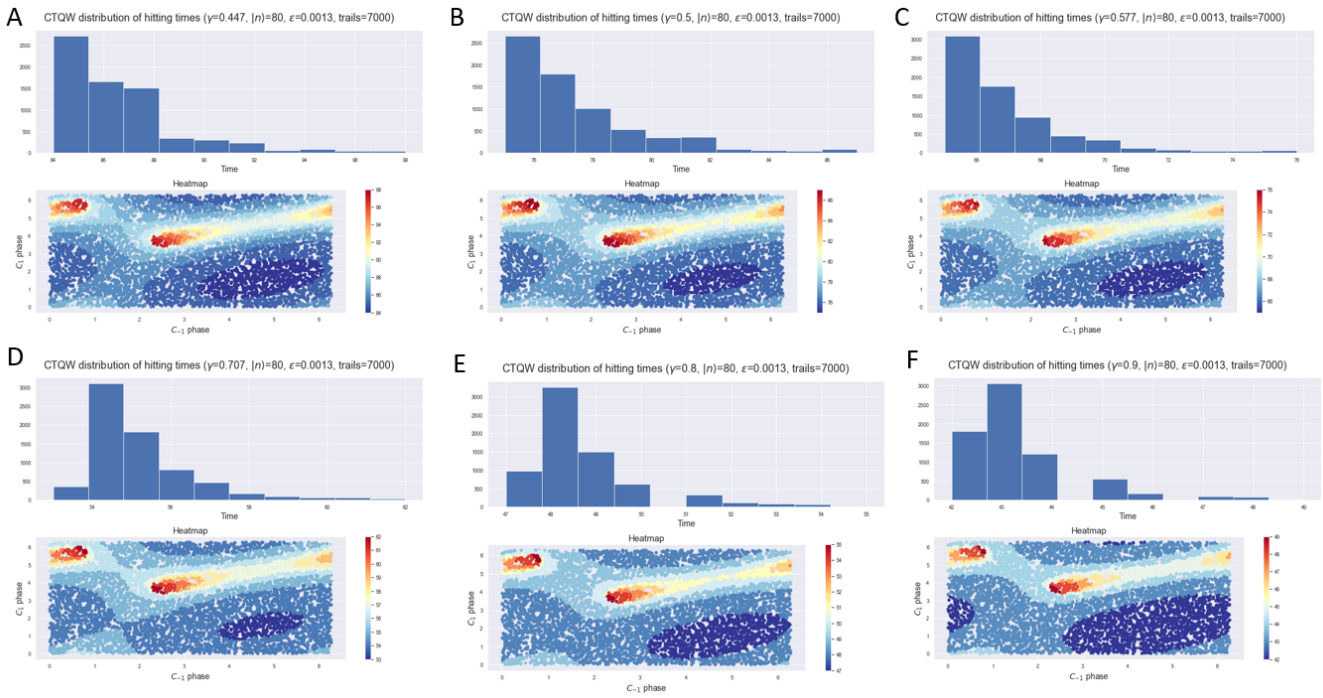

Figure 7: Distribution of detection times for different initial configurations of the form: $[0, ...C_{-1}, 1, C_1, ...0]$. We parameterize $C_{-1} = \exp i\phi_{-1}$ and $C_1 = \exp i\phi_1$. Each plot corresponds to different kicking strengths ($2\gamma_0$), the same target state $|n\rangle = 80$, and detection strength $\epsilon = 0.0013$. The heatmap shows the distribution of hitting times with the initial phases $\{\phi_{-1}, \phi_1$. Thse plots can be used to design initial states to optimize the detection times.

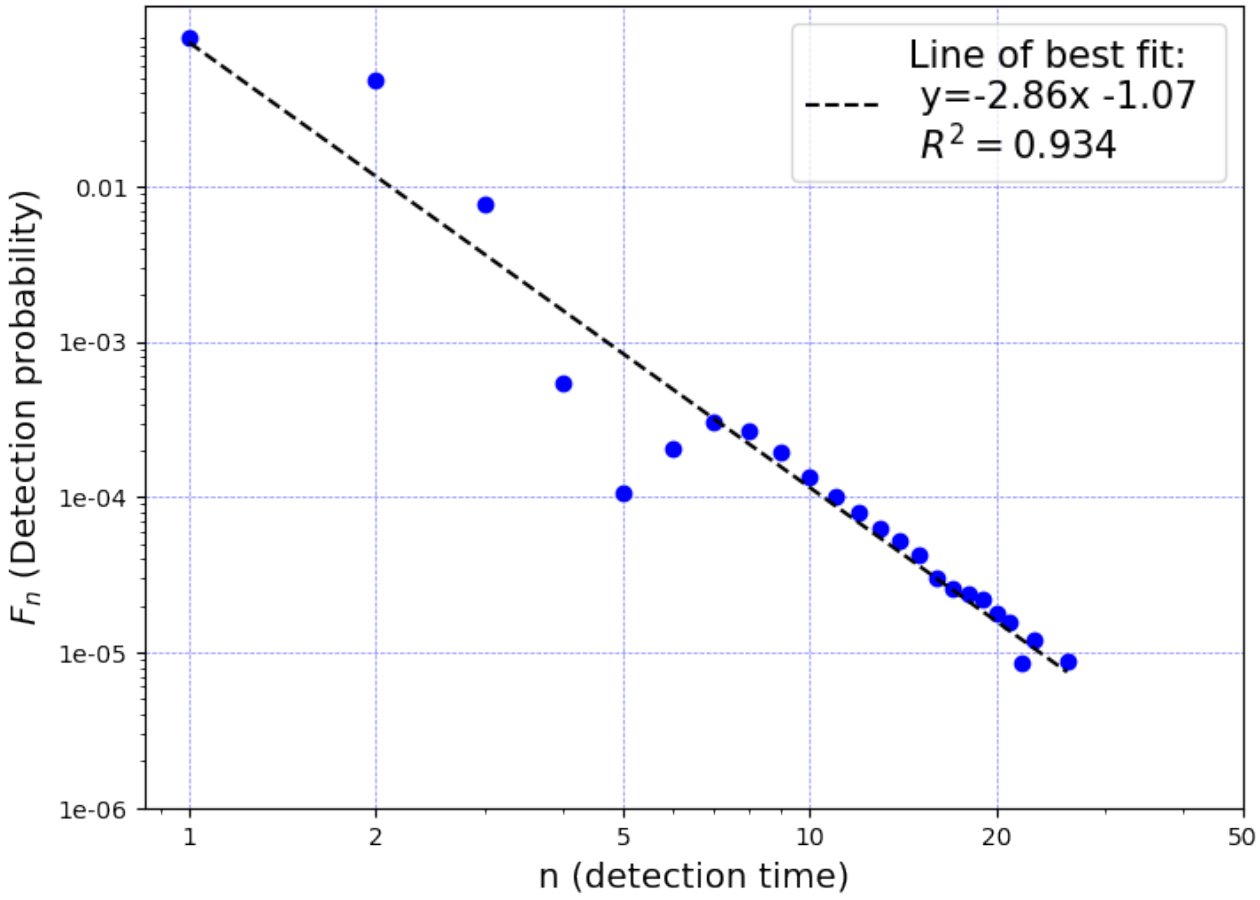

Figure 8: Detection time distribution for a QKR at resonance using the renewal equation. We detection the probability of measuring the particle at the origin after each sampling time (Here, we use $\tau = 3$). We obtain a power law decrease with an exponent of ≈ -2.86. To obtain points beyond detection time > 28, we need to solve larger systems, for higher sampling times. Such a behaviour was first characterised in [19]

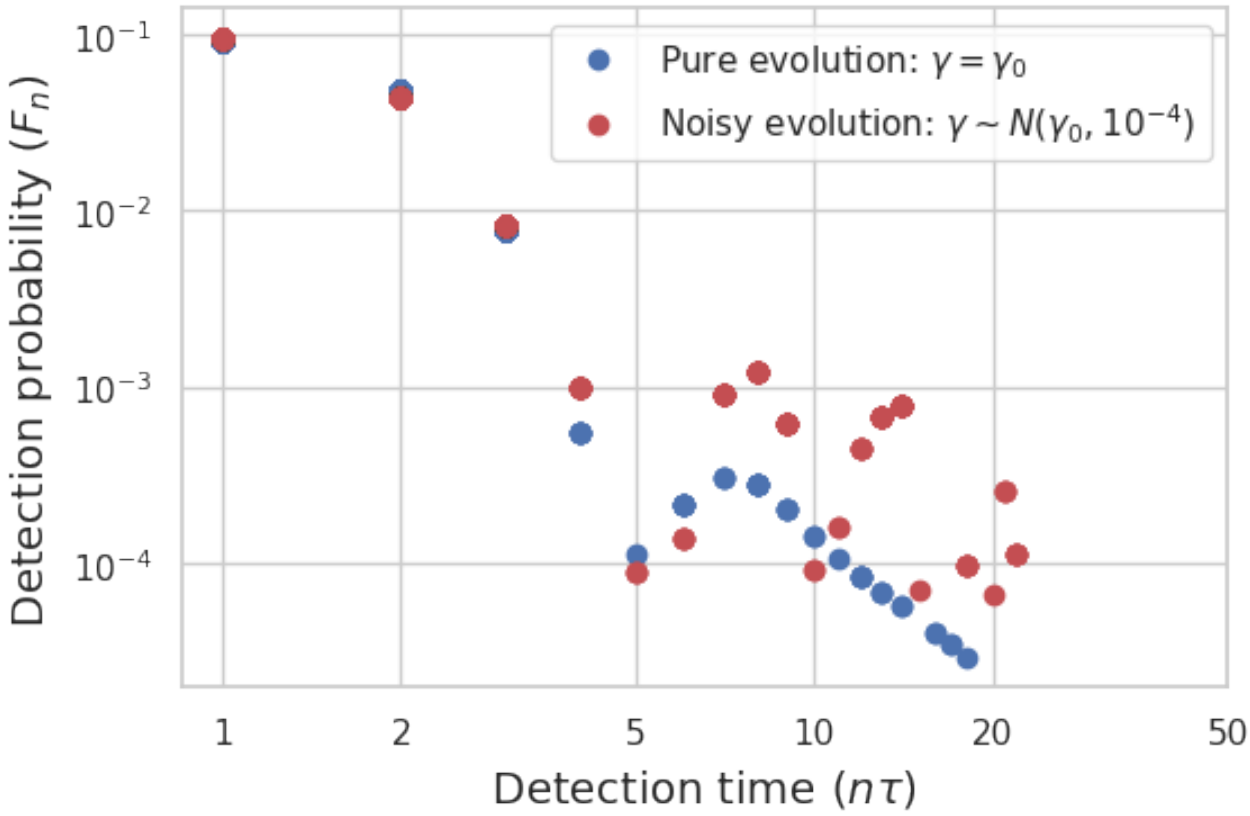

Figure 9: Detection time distribution for a QKR at resonance when the kicking strength is coherent and when sampled from a narrow Gaussian distribution with mean $\gamma = \pi/6$ and $\sigma = 0.01$. We observed strong oscillations for noisy kicks. Such systems can be studied for longer measurement times to verify if they also exhibit quantum advantage.

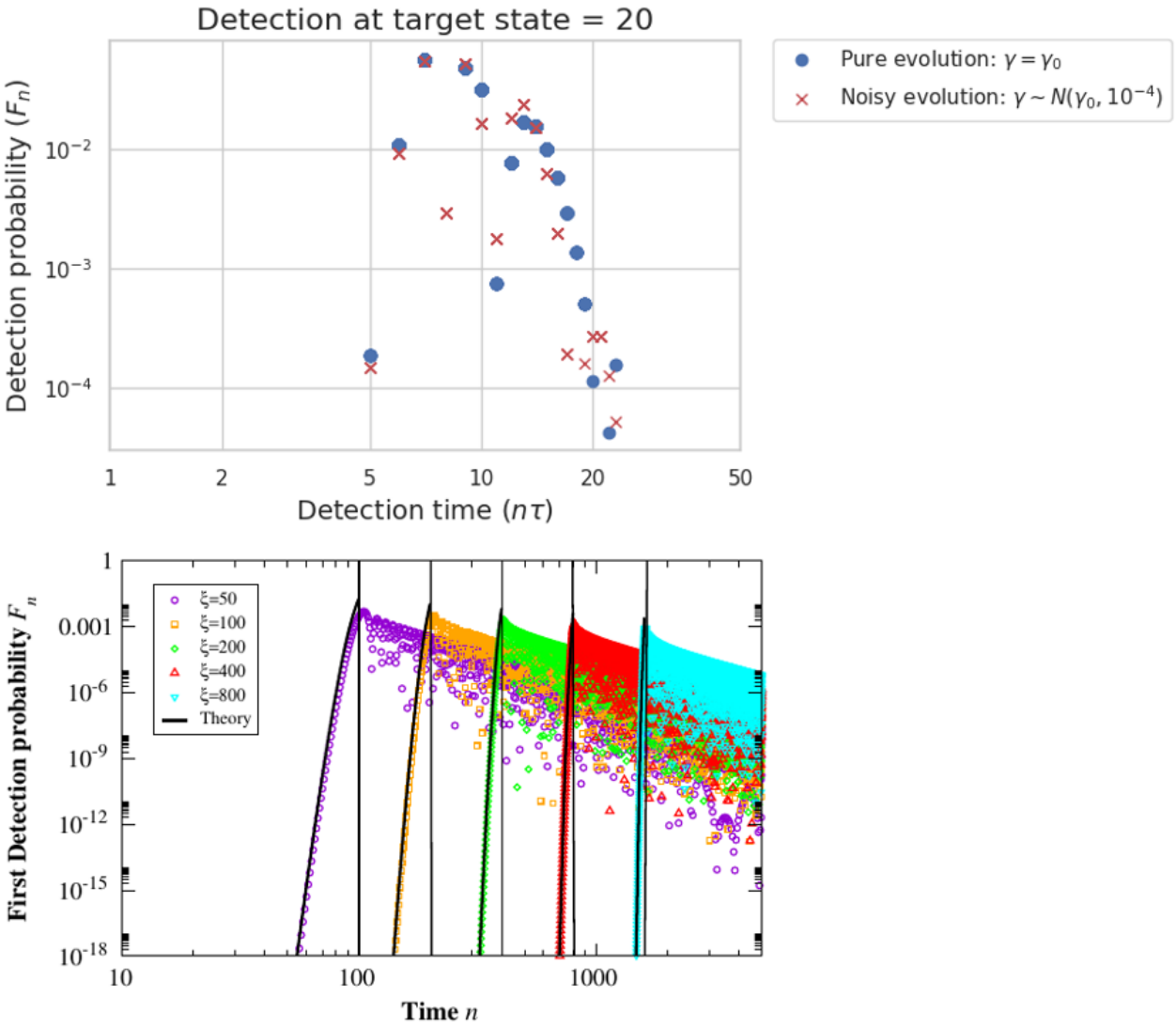

Figure 10: Detection time distribution for a target state i.e the detector is placed at the target state and the initial state is $|\psi(0)\rangle = |0$ (Top: $|n\rangle = 20$) for noisy and coherent kicks. The second graph is obtained from a more comprehensive study [19]. ξ represents the target state. A universal behavior for detection times can be observed by rescaling F_n/ξ in the bottom plot.